Autonomous high-temperature healing of surface cracks in Al$_2$O$_3$ containing Ti$_2$AlC particles

Boatemaa, Linda; Bosch, Myrthe; Farle, Ann Sophie; Bei, Guo Ping; van der Zwaag, Sybrand; Sloof, Willem G.

Important note
To cite this publication, please use the final published version (if applicable).
Please check the document version above.

ORIGINAL ARTICLE

Autonomous high-temperature healing of surface cracks in Al₂O₃ containing Ti₂AlC particles

Linda Boatemaa[1] | Myrthe Bosch[1] | Ann-Sophie Farle[1] | Guo-Ping Bei[1] |
Sybrand van der Zwaag[2] | Willem G. Sloof[1]

[1]Department of Materials Science and Engineering, Delft University of Technology, Delft, The Netherlands

[2]Faculty of Aerospace Engineering, Delft University of Technology, Delft, The Netherlands

Correspondence
Linda Boatemaa, Department of Materials Science and Engineering, Delft University of Technology, Delft, The Netherlands.
Email: l.boatemaa@tudelft.nl

Abstract

In this work, the oxidation-induced crack healing of Al₂O₃ containing 20 vol.% of Ti₂AlC MAX phase inclusions as healing particles was studied. The oxidation kinetics of the Ti₂AlC particles having an average diameter of about 10 μm was studied via thermogravimetry and/or differential thermal analysis. Surface cracks of about 80 μm long and 0.5 μm wide were introduced into the composite by Vickers indentation. After annealing in air at high temperatures, the cracks were filled with stable oxides of Ti and Al as a result of the decomposition of the Ti₂AlC particles. Crack healing was studied at 800, 900, and 1000°C for 0.25, 1, 4, and 16 hours, and the strength recovery was measured by 4-point bending. Upon indentation, the bending strength of the samples dropped by about 50% from 402 ± 35 to 229 ± 14 MPa. This bending strength increased to about 90% of the undamaged material after annealing at 1000°C for just 15 minutes, while full strength was recovered after annealing for 1 hour. As the healing temperature was reduced to 900 and 800°C, the time required for full-strength recovery increased to 4 and 16 hours, respectively. The initial bending strength and the fracture toughness of the composite material were found to be about 19% lower and 20% higher than monolithic alumina, respectively, making this material an attractive substitute for monolithic alumina used in high-temperature applications.

KEYWORDS
alumina, MAX phase, oxidation kinetics, self-healing, Ti₂AlC

1 | INTRODUCTION

Sintered alumina is an attractive material for high-temperature applications due to its heat, corrosion, and wear resistance.[1,2] The strength and hardness of this material is maintained up to high temperatures.[3] However, the brittle nature of Al₂O₃ results in a poor damage tolerance and hence limits its use.[4] Small cracks or defects can readily lead to abrupt fracture; however, autonomous repair of small crack damage may postpone or even mitigate failure. It has been reported that crack damage in alumina can be healed by high-temperature oxidation of dispersed SiC particles.[5–10] Recently, it has also been shown that dispersed TiC particles can effectively heal cracks in alumina[11,12] by the formation of TiO₂ and even require much lower oxidation temperatures than SiC particles. Ideally, in an Al₂O₃, matrix cracks should be healed by Al₂O₃ forming healing particles such as Al, but this is not feasible due to its low-melting temperature of 660°C.[13] Hence, this

work explores the possibility of oxidation-induced repair of crack damage in Al_2O_3 by dispersed Ti_2AlC MAX phase particles which forms both Al_2O_3 and TiO_2 upon oxidation.

MAX phase ceramics are a group of ternary carbides and nitrides which exhibit the properties of both metals and ceramics and are very promising materials for high-temperature applications.[14]

They exhibit a unique combination of thermal, mechanical, and electrical properties,[15] which arises from its crystallographic structure. MAX phase materials have an atomic layered hexagonal crystal structure[16] in which ceramic layers (MX) alternate with layers of pure metals (A), where M is an early transition metal, X is either a carbon or a nitrogen, and A (typically Al or Si) is usually a group IIIA or IVA element.[16] The general formula is $M_{n+1}AX_n$, where n equals 1, 2, or 3. The MX layer provides the material with high-temperature strength and stiffness characteristic of ceramics, while the relatively weakly bonded A layer provides the material with toughness, ductility, electrical, and thermal conductivity values commonly found in metals.[17,18] Dislocations in these materials glide along the basal planes, and plastic deformation occurs by a combination of kink and shear band formation, thereby rendering the material damage tolerant.[16]

Of the ternary carbides, the Ti_2AlC phase has generated a lot of interest since its density is lower than that of other ternaries and it is the most stable phase in the Ti-Al-C system,[19] making it attractive for lightweight high-temperature applications. Bulk oxidation of Ti_2AlC has been studied isothermally at high and low temperatures.[18,20] Due to the selective diffusion of Al, a protective scale consisting of a continuous inner Al_2O_3 layer and a discontinuous outer TiO_2 (rutile) layer is formed.[20] The fast diffusion of Al is due to the energy barrier for migration of Al being lower than that of Ti, and therefore, Al diffusion is favored during vacancy migration in Ti_2AlC.[21] To add to this, the bonding between Ti and C is strongly covalent, whereas the bonding between Ti and Al is relatively weak.[22] Hence, the mobility of Ti and C atoms by vacancy-assisted diffusion is retarded much more than that of Al atoms.[23] The combined effects results in preferential migration of Al atoms in the substrate leading to the formation of a protective α-Al_2O_3 scale.

Cracks in bulk Ti_2AlC have been shown to self-heal when the material is annealed at high temperatures in an oxygen-rich environment. Multiple crack healing has also been demonstrated[24] making Ti_2AlC a viable healing agent for the (extrinsic) healing of surface cracks in ceramics.[7,25–27] The suitability of Ti_2AlC as a healing agent in alumina is in line with the generalized 6-point selection process for healing agents in inert oxide ceramics presented in ref. 13: (i) Ti_2AlC has sufficient high melting temperature of 1625°C[28] making it sinterable, (ii) it expands with a relative volume expansion of about 57% upon formation of its oxides, and (iii) its coefficient of thermal expansion (CTE) is 8.2×10^{-6} K^{-1},[29] this is,

comparable to that of alumina which ranges between 7.1 and 8.3×10^{-6} K^{-1},[30] therefore only mild thermal stresses generate upon cooling from the sintering temperature. After annealing the Ti_2AlC healing particles under appropriate conditions, both TiO_2 and Al_2O_3 are formed. The latter is the same as the matrix material and will, therefore, exhibit the same physical and mechanical properties, hence only the viability of TiO_2 as a healing oxide is assessed hereafter. (iv) TiO_2 has a melting temperature of 1857°C, that is, it is still a solid when the composite is operated as high as 1400°C, (v) the work of adhesion between TiO_2 and Al_2O_3 is higher than that between atoms of Al_2O_3 implying a strong bond of the oxide to the matrix[13] Lastly, due to the difference in CTE, tensile stresses may be generated in the TiO_2 healing layer, but the calculated value is well below the tensile strength of Al_2O_3.[13] Hence, Ti_2AlC passes the primary selection criteria as a suitable healing agent for Al_2O_3, and this potential suitability is, thus, investigated experimentally in this study.

The $Ti_2Al_{0.5}Sn_{0.5}C$ is another MAX phase which has been used as a particulate inclusion to heal surface cracks in Al_2O_3.[31] The composite contained 20 vol.% of the healing particles and complete flexural strength recovery was observed after annealing at 700°C for 48 hours or at 900°C for 0.5 hour for samples containing cracks typically 300 μm long and 0.5 μm wide. After annealing, SnO_2, TiO_2, and Al_2O_3 were detected close to the sample surface, while SnO_2 was not detected deeper inside the crack gap.

The current work concerns the synthesis of Ti_2AlC MAX phase and a study of its isothermal and nonisothermal oxidation behavior. The recovery of the fracture strength of Al_2O_3 composites containing 20 vol.% of the Ti_2AlC particles is investigated by micro indentation, subsequent high-temperature annealing, and finally 4-point bending at room temperature.

2 | EXPERIMENTAL PROCEDURE

The Ti_2AlC was first synthesized from elemental powders of Ti (5 μm, 99.5% purity from Chempur, Germany), Al (5 μm, 99.5% purity from Alfa Aeaser, Germany), and TiC (5 μm, 99.5% purity from Chempur, Germany). The powders were mixed in molar compositions of 1.15:1.1:0.85, respectively, with zirconia balls in a Planetary ball mill PM 100 (Retsch, Germany). A combination of zircona balls with 10 and 5 mm diameter was used to attain an even mixture with a powder to ball mass ratio of 2:1. The mixing profile was 150 rpm for 4 hours in argon with an on and off period of 20:10 minutes. The mixed powders were packed into 40-mm carbon molds and reactively sintered by Spark Plasma Sintering (SPS) using a HP D 25 SD furnace (FCT Systeme, Germany). The samples were heated up at 60°C/min from ambient temperature and held at 1350°C for 2 hours under vacuum. A pressure of 5 MPa was applied from the start until 20 minutes after

1350°C was reached, and then the pressure was increased to 50 MPa for 1 hour and 40 minutes. The samples were cooled to room temperature at 100°C/min.

The MAX phase tablets were fragmented using TiN-coated drill bits and crushed with a heavy press. The pieces were milled in the planetary ball mill at 300 rpm in isopropanol for 10 hours with an on and off period of 20:10 minutes. To powder the material to submicron size range, tungsten carbide balls (with 20 and 10 mm diameter) were used. And for a narrow distribution of the particles, a size separation was done by suspending the powders in isopropanol. Powders that sunk to the bottom within 1 hour were re-milled until an acceptable size was achieved. The size distribution of the milled particles was measured by laser diffraction using a Microtrac 3500 (Microtrac).

Subsequently, the composite was made using high purity (4 N) Al_2O_3 powder (Sumitomo Chemical, Tokyo, Japan) with an average particle size of 0.2 μm and 20 vol.% of the prepared Ti_2AlC powder. The powders were mixed in with isopropanol with a Turbula mixer T2C (Willy A. Bachofen, Switzerland) for 24 hours using zirconia balls (with 10 and 5 mm diameter). After drying, the cake was grounded and passed through a 200 μm sieve before sintering. The thoroughly mixed powder was packed into a 40 mm mold and heated at 20°C/min up to 1300°C and held for 10 minutes in argon under 50 MPa in the SPS furnace. After sintering, the system was cooled naturally by lifting up the pistons to avoid thermal shocking of alumina. The density of the composite was measured by the Archimedes method using an analytical balance (Mettler Toledo AG-204, Switzerland) according to ASTM B 311-93.[32]

The oxidation behavior of the synthesized pure Ti_2AlC particles was studied isothermally and nonisothermally by thermogravimetric and/or differential thermal analysis (TGA or DTA) using a SETSYS Evolution 16/18 simultaneous thermal analyzer (Setaram, France). This thermal analyzer is equipped with an S-type thermocouple which is operable up to 1700°C. The Ti_2AlC powder (20 ± 1 mg) was put into an Al_2O_3 crucible (100 μL), and the furnace was heated from room temperature to 1400°C with 4°C/min under synthetic air flowing at 8.33×10^{-7} m^3/s, that is, 50 mL/min at standard conditions (ie, at 293 K, and 1 bar). For the isothermal experiments, the samples were heated in the furnace from room temperature with 10°C/min under pure N_2 (with $H_2O < 10$ ppm) supplied at 8.33×10^{-7} m^3/s at standard conditions. When the desired temperature was reached, the volume of N_2 was reduced by 20% and replaced by O_2, thereby generating synthetic air in the furnace. After the 10 hours hold, the sample was cooled down with 10°C/min under pure N_2 flowing at 8.33×10^{-7} m^3/s at standard conditions. The mass change curves were corrected for buoyancy by performing a thermogravimetric measurement under the same conditions but using an empty crucible.

The oxides formed during isothermal oxidation of the Ti_2AlC particles were analyzed with X-ray microanalysis (XMA) and/or X-ray diffraction. A JSM 6500F (JEOL, Japan) scanning electron microscope (SEM) equipped with an energy dispersive spectrometer (EDS) for X-rays was used for the XMA. The EDS is an UltraDry detector (30 mm²) with Noran System Seven software package (Thermo Fisher Scientific) for data acquisition and analysis. The SEM was also used for observing the shape and size of the MAX-Phase particles, the microstructure of the composite, the size of the indents, and the cracks. After healing the products that filled, the cracks were analyzed by XMA.

The phase purity and composition of the samples were analyzed by X-ray diffraction using a Bruker D8 Advance diffractometer (Bruker, Germany) equipped with a graphite monochromator. Diffractograms were recorded with Co or Cu Kα radiation in the 2θ range of 20-90° with a step size of 0.034° and a dwell time of 2 seconds. The diffractograms were processed with the accompanying Diffrac. EVA 4.1 Bruker software.

To study the strength recovery of the alumina with Ti_2AlC particles, SPS-produced samples were machined to $3.0 \times 4.0 \times 26.0$ mm rectangular bars with beveled edges. The surfaces of the bars were polished with a 1-μm diamond suspension in the final step. Cracks were introduced at the center of the bar by means of Vickers' indentation using a Zwick/Z2.5 hardness tester (Zwick, Germany) under displacement control mode of 0.5 μm/s with a maximum load of 30 N held for 20 seconds at load. The indenter was oriented such that the radial cracks were perpendicular to the tensile stress induced during 4-point bending. Annealing to repair the cracks was carried out in a Carbolite TZF 17/600 furnace (Carbolite Gero, UK) at temperatures ranging from 800 to 1000°C for 0.25, 1, 4, and 16 hours in air. The furnace is equipped with an S-type thermocouple close to the center of the furnace, thereby measuring the true sample temperature in the middle of the furnace.

The bending tests were performed at room temperature using a 4-point self-aligning stage with a 20/10 mm span and hardened steel rollers with 2 mm diameter.[12] The stage was mounted on Instron 5500R (Instron Corporation) material testing frame. A 10 kN load cell was used and the cross-head was displaced at a velocity of 0.5 mm/min. The bar specimen was placed such that its center coincided with the middle of the spans.

3 | RESULTS AND DISCUSSION

3.1 | Synthesis of Ti_2AlC particles and alumina composite

The microstructure of the synthesized Ti_2AlC is shown in Figure 1, the light gray areas are the Ti_2AlC MAX phase, and the darker areas are pores and impure phases. X-ray

diffraction and X-ray microanalysis of different samples showed that it was mostly high-purity single-phased Ti_2AlC, while a few samples had small patches of Ti_3AlC, TiC, and/or Ti_3AlC_2 as impurities (Figure 2).

The formation of the impurities is not fully controlled and understood at this point, but is thought to be related to the melting of the aluminum powder during the sintering process.

After powdering the Ti_2AlC, the particle size distribution ranged between 2 and 23 μm with an average size of
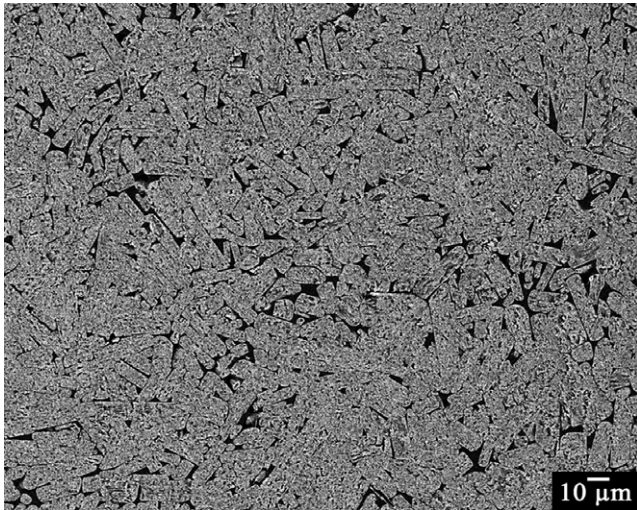

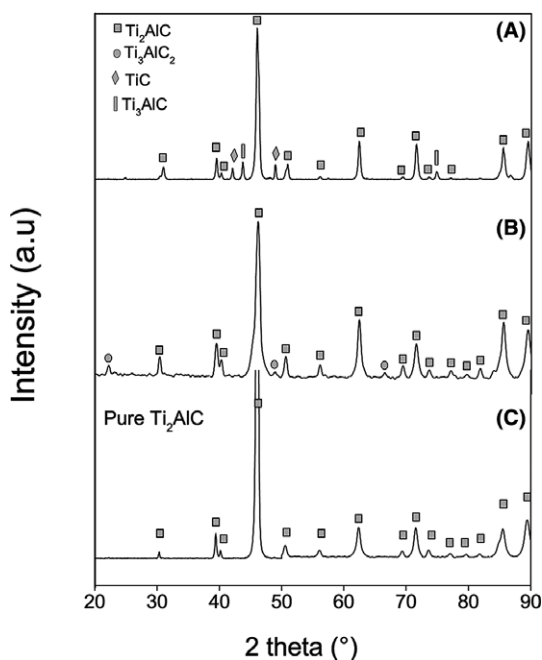**FIGURE 1** Microstructure of the sintered Ti_2AlC pellet

FIGURE 2 Diffractograms showing purity levels of the sintered material (A) Ti_2AlC with TiC and Ti_3AlC impurities (B) Ti_2AlC having Ti_3AlC_2 impurities and (C) Pure Ti_2AlC

about 10 μm. The particles as observed with SEM were irregular, platelet, cylindrical, or whisker shaped depicting the underlying laminar structure of the MAX phase.

It was observed that the elongated MAX phase particles in the composite were evenly dispersed as shown in Figure 3. At a relatively low magnification, these particles appear to be aligned perpendicular to the direction of the applied pressure during sintering; however, at a high magnification, this alignment is not apparent. XRD and XMA analysis of the composite showed that no chemical reaction had taken place between the healing particles and the matrix, implying that the particles were intact and ready to be used for crack healing when exposed to the appropriate conditions.

3.2 | Oxidation kinetics of the Ti_2AlC particles

When Ti_2AlC powder is exposed to an oxidative environment at high temperatures, Ti and Al oxidize eventually to rutile (TiO_2) and alumina (Al_2O_3), respectively. To identify which oxide is formed at what temperature a combined nonisothermal TGA and DTA of the Ti_2AlC powder in dry synthetic air was performed from room temperature to 1400°C with 4°C/min. The results presented in Figure 4 show that there are 2 main peaks one at 580 and another at 910°C, which are likely to be associated with the formation of TiO_2 and Al_2O_3, respectively.

To identify which material is formed at the first and second peak in Figure 4, nonisothermal oxidation experiments were executed with the Ti_2AlC powder in dry synthetic air up to 760 and 980°C. X-ray diffraction of the oxidized powder heated up to 760°C indicates that about 40% of the starting material remains unoxidized and equal amounts of rutile and anatase (TiO_2) were identified
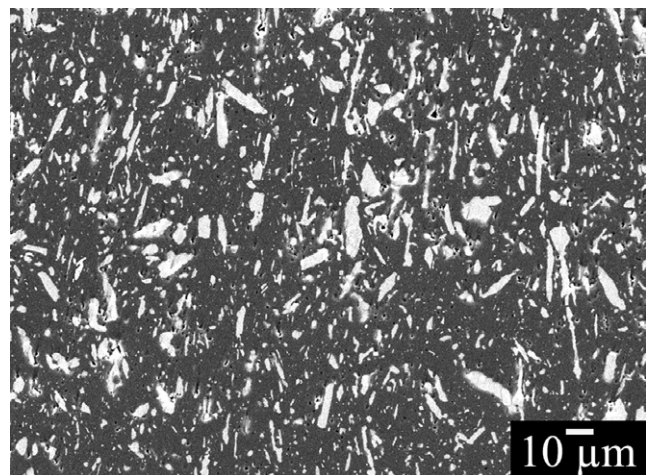

FIGURE 3 Sintered composite showing homogenous distribution of Ti_2AlC particles (light) in alumina (dark)

including a little amount of TiAl. When heating the Ti_2AlC powder up to 980°C, it is fully converted into TiO_2 and Al_2O_3. Thus, the remaining powder and any intermediary phase (eg, anatase and TiAl) are converted to rutile and corundum (α-alumina) in the second peak; cf. Figure 4.

Also, isothermal thermogravimetric oxidation experiments were performed with the Ti_2AlC powder in dry synthetic air for 10 hours in the temperature range of 560-1060°C (Figure 5). After each annealing treatment, the oxidation products were identified by XRD. The oxidation rate of the Ti_2AlC powder decreases with time due to the increasing thickness of the oxide shell which acts as a strong diffusion barrier as shown in Figure 5. Above 800°C, the oxidation proceeds very fast with all Ti_2AlC being converted in 2 hours at 860°C and in 20 minutes at 960 and 1060°C. However, at low temperatures, the reaction proceeds at the same rate as at the high temperatures for the first few minutes before deviating to grow at a much slower rate. Thus, after 10 hours, 80% of the Ti_2AlC powder kept at 760°C had been transformed, while at 660 and 560°C, only 30% and 40% had been transformed, respectively.

At 560 and 660°C, only rutile and TiAl were detected with large amounts of the starting material (Figure 6). At 760°C, alumina and rutile are detected with some amount of the MAX phase. At 860°C and above, only rutile and alumina are detected. The formation of TiAl is due to simultane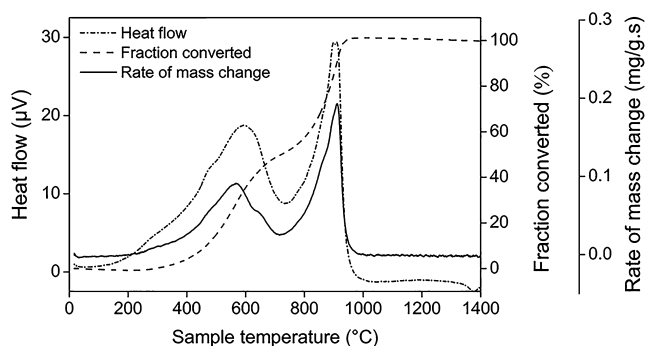ous selective oxidation of carbon (transformed into CO_2 as observed with mass spectrometry) and formation of TiO_2.

A deviation in the rate of the oxide growth at 660°C is observed after about 20 minutes of exposure leading to only 30% of the material being converted, while at 560°C, almost 40% of the powder was transformed at the end of 10 hours of oxidation period (Figure 5B). This irregularity has also been reported[23] and is likely due to the initial formation of anatase at 560°C (according to XRD results of the nonisothermal oxidation) which grows faster[23] and is a porous and nonprotective oxide.[33] At higher oxidation temperatures (660°C and above), rutile is formed which hinders "fast oxidation" of the underlying material.[23]

3.3 | Mechanical properties of the Al_2O_3-Ti_2AlC composite

Surface cracks were introduced in the composite material by Vickers indentations with varying load. Application of a load of 20 N resulted in a crack of about 80 ± 5 μm in length (2c); at the same load, the crack registered in the alumina containing 20 vol.% of TiC composite was 100 ± 8 μm.[11] The relationships between load and crack length for an Al_2O_3 matrix containing either Ti_2AlC or TiC are plotted in Figure 7. From these data, the fracture toughness of the alumina with 20 vol.% TiC was evaluated to be 4.3 ± 0.1 MPa $m^{1/2}$,[11] while that of the alumina with Ti_2AlC is 4.9 ± 0.5 MPa $m^{1/2}$, indicating an increased resistance to fracture. This observed toughening behavior is brought about by the mechanical behavior and properties of both the matrix and the incorporated healing agent.[34] However, the initial average bending strength of the Al_2O_3 with 20 vol.% Ti_2AlC is smaller than that of the Al_2O_3 with 15 vol.% TiC composite, 415 ± 28 vs 526 ± 90 MPa.[12] The size of the TiC-healing particles is on average much smaller than that of Ti_2AlC, that is, 2 vs 10 μm. It can be assumed that the strength of the composite decreases as the size of the healing particles increases.[34]

Depending on the direction of a crack and the local stress intensity factors, a crack may be bridged, deflected, or arrested (Figure 8), as it approaches a second-phase component.[37] The MAX phase exhibits some ductility

FIGURE 4 Oxidation kinetics of Ti_2AlC powder in air at 4°C/min: heat flow, fraction converted, and rate of mass change (recorded mass change differentiated) vs temperature
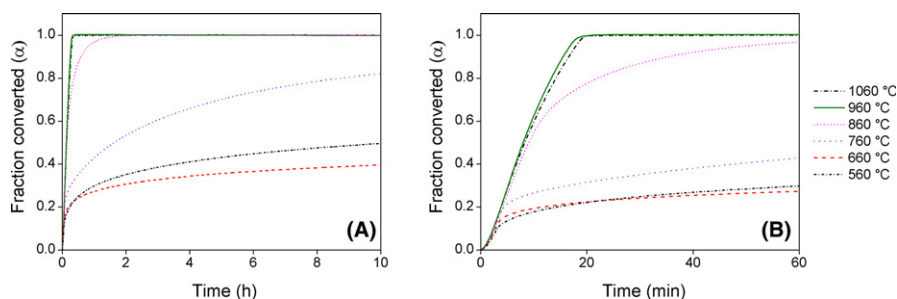
FIGURE 5 A, Isothermal conversion of Ti_2AlC at different oxidation temperatures for 10 h in dry synthetic air as determined from thermogravimetric analysis; B, enlargement showing the first hour [Color figure can be viewed at wileyonlinelibrary.com]
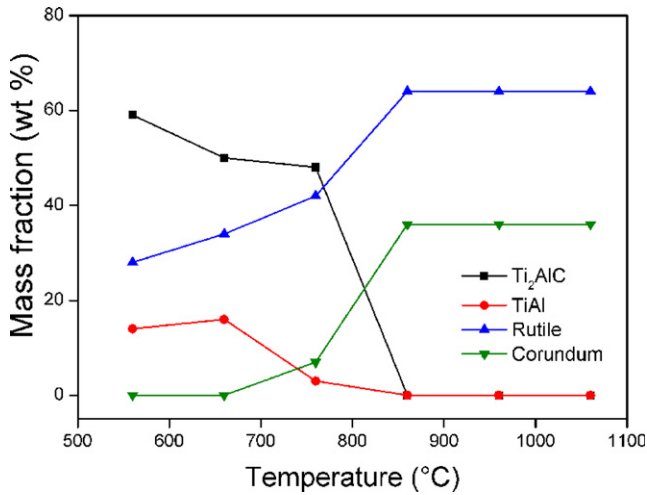
FIGURE 6 Mass fractions of the Ti$_2$AlC starting material and the oxidation products at different temperatures after 10 h of oxidation in dry synthetic air [Color figure can be viewed at wile yonlinelibrary.com]
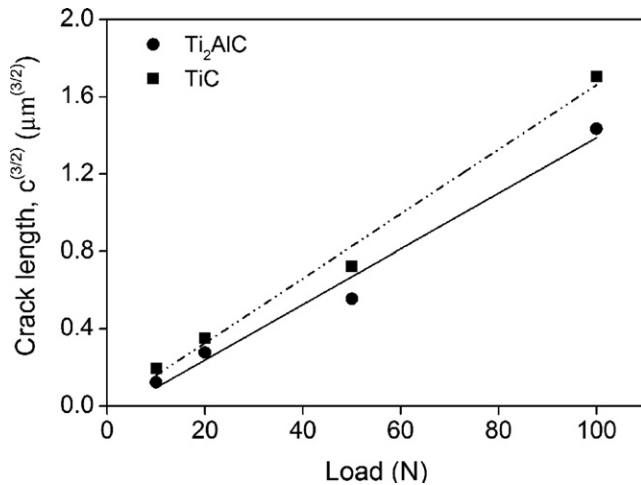

FIGURE 7 Comparison of the length of Vickers' indentation induced cracks with length c generated in Al$_2$O$_3$/Ti$_2$AlC and Al$_2$O$_3$/TiC composite[12]

FIGURE 8 Toughness enhancement mechanisms of Ti$_2$AlC in Al$_2$O$_3$. SEM images (A) cracks blunted by particle, (B) and (C) cracks intersecting a particle or diverted along the particle-matrix interface

leading to absorption of energy at the tip of an approaching crack, thereby blunting the crack tip (Figure 8A). Its whisker-like shape may bridge the cracks (Figure 8B,C) causing a significant shielding effect.[37]

In contrast, crack-driving forces are amplified in the wake of softer particles leading to anti-shielding effects.[38] Finally, micromechanical models for crack particle interaction in brittle particulate composites[38] have shown that a crack in the matrix is attracted to the particles if the elastic modulus of the particles is lower than that of the matrix. In this case, the elastic modulus of Ti$_2$AlC is 277 GPa,[39] and it is lower than that of alumina, which is between 380 and 410 GPa,[40] hence cracks are attracted to the Ti$_2$AlC particles. It is worth pointing out that growing of cracks through the particles or along the matrix-particle interfaces
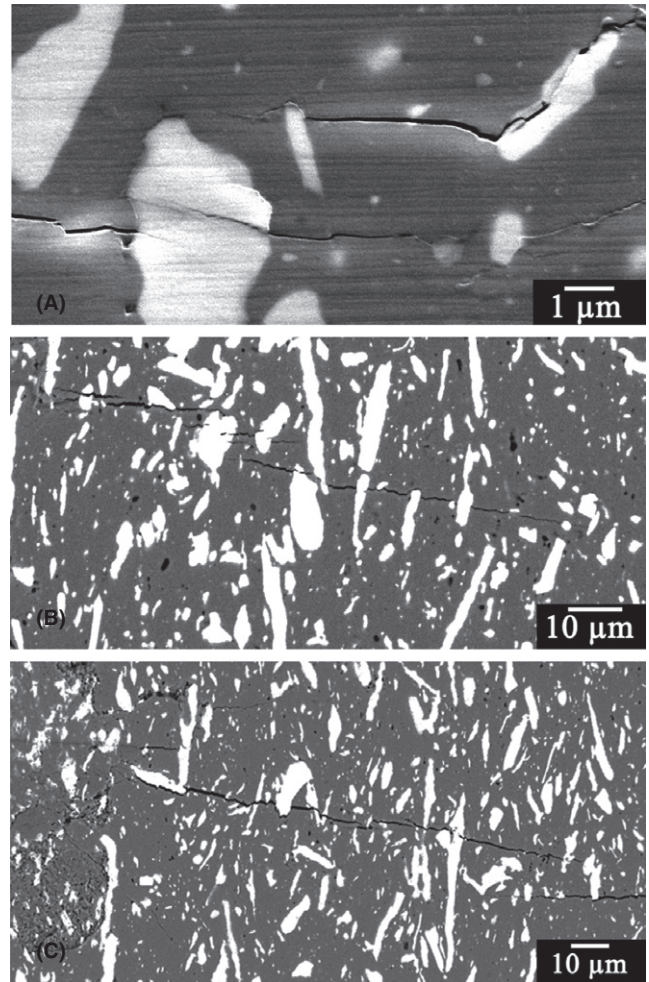
are acceptable as in both cases the particle content is exposed directly to the crack volume which is essential for the self-healing reaction to take place.

3.4 | Strength recovery the Al$_2$O$_3$-Ti$_2$AlC composite

The strength values of the virgin composite samples, the damaged samples, and the healed composites as measured by 4-point bending tests are shown in Figure 9. It is noted that the long axes of the elongated Ti$_2$AlC healing particles are aligned perpendicular to the sample surface at which the load is applied. Each data point represents an average of 8 samples. The initial average strength of the composite was 415 ± 28 MPa.

For the indented samples, the strength decreased to 229 ± 14 MPa which is about 50% of the initial strength. After annealing at 1000°C for 15 minutes, the strength significantly increased to 354 ± 29 MPa, which is about 90%

of the initial strength. After 1 hour at the same temperature, full strength was almost regained at 97% and after 4 hours complete strength was recovered. There was no significant difference in the strength regained for samples kept at 900°C for 1 and 4 hours as strength regain of 94% and 95% was registered, respectively. Similarly, at 800°C, the strength recovered was 92% and 90% for 4 and 16 hours, respectively. Most healed samples fractured next to the healed crack, indicating a strong adhesion between the healing oxide and the Al_2O_3 matrix. However, samples with cracks that were not fully healed fractured along the original crack path, since the unfilled parts of the crack acts as initiation sites.

Surface observations of the healed samples by SEM in the as-annealed state (Figure 10A) showed that upon annealing at 800°C for 4 hours, there was significant local volume expansion at the site of some Ti_2AlC particles (as expected), but surprisingly not all particles showed this volume expansion. This may be because the basal planes which enhance outward diffusion of the elements may be aligned or tilted away from the surface of the sample.
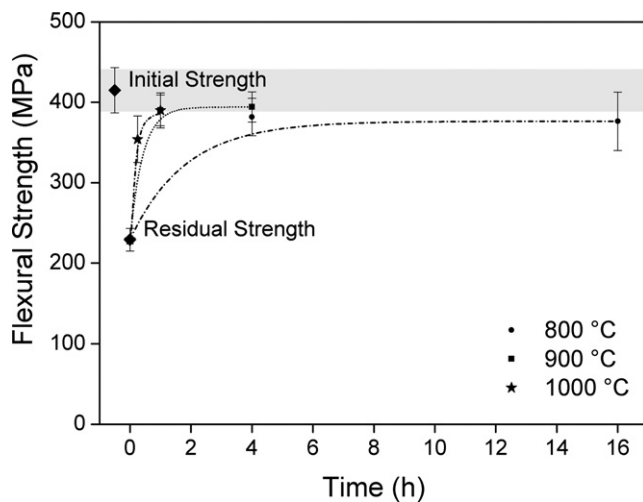

FIGURE 9 Flexural strength of studied materials attained by 4-point bending

Upon polishing the sample, it is clear that crack filling starts at the particles intersected by the crack, and it is also clear that the cracks are not fully filled (Figure 10B). This is somewhat remarkable given the high strength recovery of 92%. The high strength recovery is attributed to bridging of the gaps by oxides formed locally from particles exposed to the crack. Recent work on in situ monitoring on monolithic Ti_2AlC material[41] proved that even for reactive materials crack filling can occur well below the external surface. After annealing at 900°C for 1 hour, cracks were found to be seemingly fully filled with TiO_2 and small amounts of Al_2O_3. Upon annealing at 1000°C for 1 hour, cracks were found to be fully filled with Al_2O_3 and TiO_2. Figure 11 shows the same area of a sample captured before oxidation (A), after oxidation at 1000°C for 1 hour (B), and after the surface is polished to show the extent of filling attained (C). The completely filled crack path in the healed sample can be identified as a line filled with TiO_2 (light) and interrupted by Al_2O_3 (dark). The set of SEM observations clearly demonstrate the lateral expansion of the oxides formed at the healing particle into the crack which is not in direct contact with a particle. This lateral expansion of the oxides formed at the healing particles has often been assumed, but had not been demonstrated as convincingly as in this set of micrographs.

At the studied temperatures and conditions, no reaction was observed between alumina and the dispersed Ti_2AlC particles or the healing agents (TiO_2 and Al_2O_3) in the composite. Therefore, the healing ability of the Ti_2AlC particles is not in hindered in any way by an intermediary reaction. However, the rate of oxidation of the embedded particles will only be less due to the reduced reaction area in comparison with the free particles.

3.5 | Stability of the dispersed Ti_2AlC particles in the Al_2O_3 matrix

The success of the extrinsic healing approach as used in this research depends on the healing particle remaining
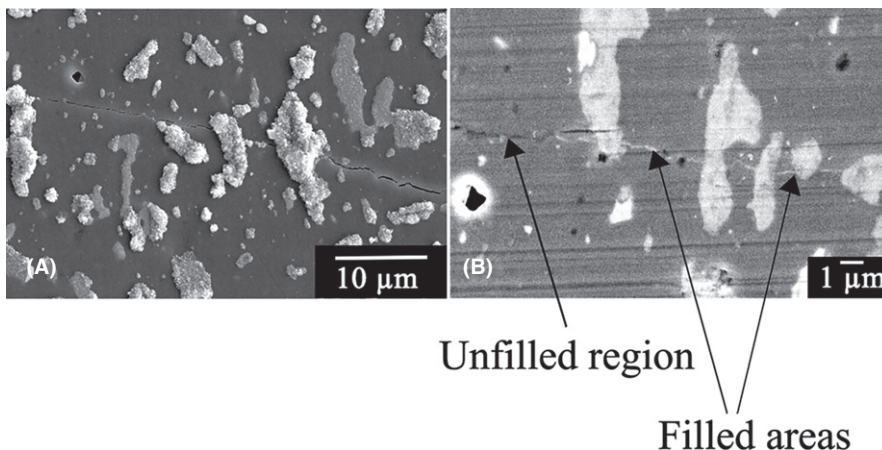

FIGURE 10 SEM images of sample kept at 800°C for 4 h (A) unpolished surface and (B) polished surface. The crack is partially filled as indicated by the arrows
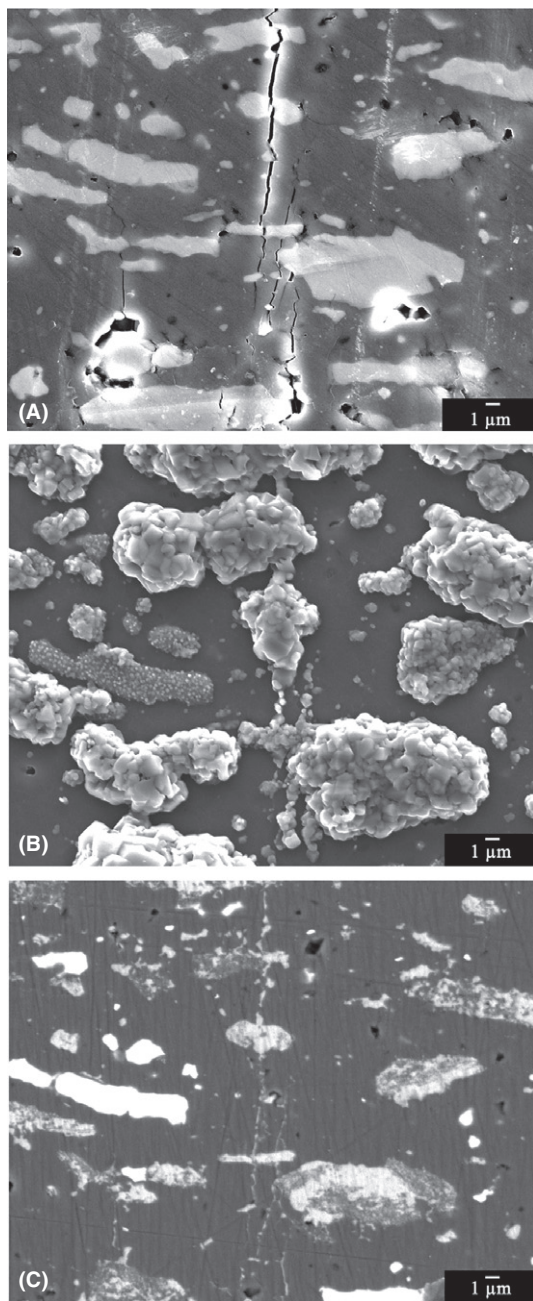
FIGURE 11 SEM images of the same crack area before and after healing at 1000°C for 1 h in air. A, Before oxidation. B, After oxidation and before polishing. C, Polished surface showing fully filled cracks

FIGURE 12 SEM cross-sectional view of the composite at 1000°C in air for (A) 64 and (B) 256 h showing the depletion of Ti and Al from the Ti_2AlC particles close to the sample surface

unaffected by the exposure conditions of the sample and not decomposing before a crack intersected the particle. Such an unprompted reaction would not only lead to a reduction or loss of the healing potential but would also induce local stresses in the Al_2O_3 matrix. This may lead to a reduction of the tensile strength and in the limit even to spontaneous crack formation. To examine the stability of the healing particles in the (nonoxygen permeable) alumina matrix cross section of undamaged samples kept at 1000°C
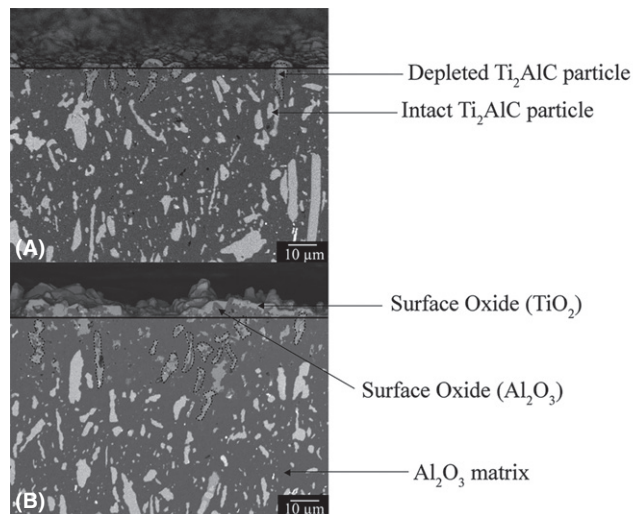
in ambient air for 64, 128, and 256 hours have been made; Figures 12A,B show the microstructures of the samples kept at 64 and 256 hours, respectively. The micrographs show that at the surface, a dense layer of Al_2O_3 formed first, but also some TiO_2 particles were observed on the surface.

Most importantly, the cross sections showed that even for the longest exposure time of 256 hours a depletion layer of <20 μm from the surface is observed. The Ti_2AlC particles within this layer do not have the stoichiometry of the starting material due to the diffusion and subsequent oxidation of Ti, Al, and/or C at the surface. Beyond this depth, XMA confirms that the MAX phase particles retain their original stoichiometry of 2:1:1 for Ti:Al:C. Although undoped fine grained alumina favors inward diffusion of oxygen,[42,43] oxidation of the MAX-Phase particles proceeds by an outward diffusion of the cations (Al^{3+} and Ti^{4+}), which is not influenced by the grain size of the matrix.[44] The depleted region is limited to about 20 μm (same as the maximum particle size), and hence alumina acts as a strong barrier against oxidation of particles embedded in the depth of the composite. The orientation of the basal planes of a particle to the surface may also influence the rate at which Al and Ti diffuse out. While it is highly desirable that the affected zone near a free surface is restricted to the diameter of the healing particle (ie, the particles do not react unless intersected by a crack), the combined effect of particle size and particle volume fraction determine and limit the amount of material to be deposited in the open crack. This dependence has been analyzed numerically in detail for healing particles in polymeric matrices,[45] but the analysis equally apply to the current case of high-temperature ceramics.

4 | CONCLUSION

The oxidation behavior of Ti_2AlC particles and its ability to heal surface cracks in Al_2O_3 containing 20% by volume was investigated. Nonisothermal analysis revealed that oxidation starts at 600°C, but the temperature for efficient healing is between 800 and 1000°C. The Ti_2AlC material is a suitable healing agent for alumina and composite materials containing 20 vol.% of 10-micron-sized Ti_2AlC particles as there was significant tensile strength recovery at 900°C for 1 hour or 1000°C for 15 minutes. At these temperatures, the cracks are filled by both TiO_2 and Al_2O_3. Healing at 800°C required 16 hours.

Most importantly, the results showed that the particles embedded in the matrix and not touching the outer sample surface did not decompose upon long-term high-temperature exposure and remained potentially active in the nonoxygen permeable Al_2O_3 matrix unless intersected by a crack. While not explored for times longer than 256 hours at 1000°C, this is a very important finding indicative that Al_2O_3 ceramics filled with Ti_2AlC particles may have long-term self-healing ability and can be of industrial relevance.

ORCID

Linda Boatemaa http://orcid.org/0000-0001-6994-2854
Guo-Ping Bei http://orcid.org/0000-0002-9315-6834
Sybrand van der Zwaag http://orcid.org/0000-0001-5085-0255
Willem G. Sloof http://orcid.org/0000-0003-1443-0813

REFERENCES

1. US-Congress. Office of technology assessment-Advanced materials by design, OTA-E-351. Washington DC: U.S. Government Printing Office; 1988.
2. Salas-Villaseñor AL, Lemus-ruiz J, Nanko M, Maruoka D. Crack disappearance by high-temperature oxidation of alumina toughened by Ni nanoparticles. Adv Mater. 2009;68:34–43.
3. Ono M, Nakao W, Takahashi K, Nakatani M, Ando K. A new methodology to guarantee the structural integrity of Al_2O_3/SiC composite using crack healing and a proof test. Fatigue Fract Mater Struct. 2007;30:599–607.
4. Yan Shi C, Kui Guo Y, Jin Zhao S, Mei Song C. Effect of healing temperature on crack-healing of Al_2O_3 toughened by SiC particles. Mater Sci Forum. 2010;650:109–14.
5. Nakao W, Abe S. Enhancement of the self-healing ability in oxidation induced self-healing ceramic by modifying the healing agent. Smart Mater Struct. 2012;21:1–7.
6. Ando K, Kim BS, Chu MC, Saito S, Takahashi K. Crack-healing and mechanical behaviour of Al_2O_3/SiC composites at elevated temperature. Fatigue Fract Eng Mater Struct. 2004;27:533–41.
7. Ando K, Ono M, Nakao W, Takahashi K, Saito S. Increase of structual integrity machined alumina/SiC using crack-healing. Ceram Trans. 2006;192:155–62.
8. Nakao W, Tsutagawa Y, Takahashi K, Ando K. Self-crack-healing ability of alumina/SiC nanocomposite fabricated by self-propagating high-temperatures synthesis. In: Lara-Curzio E, Salem J, Zhu D, editors. *Mech. Prop. Perform. Eng. Ceram. Compos. III*, 2008; p. 443–8.
9. Nakao W, Ono M, Lee SK, Takahashi K, Ando K. Critical crack-healing condition for SiC whisker reinforced alumina under stress. J Eur Ceram Soc. 2005;25:3649–55.
10. Wataru N, Shihomi A. Enhancement of the self-healing ability in oxidation induced self-healing ceramic by modifying the healing agent. Smart Mater Struct. 2012;21:025002.
11. Farle A, Boatemaa L, Shen L, Gövert S, Kok JBW, Bosch M, et al. Demonstrating the self-healing behaviour of some selected ceramics under combustion chamber conditions. Smart Mater Struct. 2016;25:084019.
12. Yoshioka S, Boatemaa L, van der Zwaag S, Nakao W, Sloof WG. On the use of TiC as high-temperature healing particles in alumina based composites. J Eur Ceram Soc. 2016;36:4155–62.
13. Boatemaa L, Kwakernaak C, van der Zwaag S, Sloof WG. Selection of healing agents for autonomous healing of alumina at high temperatures. J Eur Ceram Soc. 2016;36:4141–5.
14. Tzenov NV, Barsoum MW. Synthesis and characterization of Ti_3AlC_2. J Am Ceram Soc. 2000;83:825–32.
15. Barsoum MW, Salama I, El-Raghy T, Golczewski J, Seifert HJ, Aldinger F, et al. Thermal and electrical properties of Nb_2AlC, (Ti, Nb)$_2$AlC and Ti_2AlC. Metall Mater Trans A. 2002;33:2775–9.
16. Barsoum MW. MN+1AXN phases: a new class of solids; thermodynamically stable nanolaminates. Prog Solid State Chem. 2000;28:201–81.
17. Barsoum MW. Physical properties of the MAX phases A2 - Buschow, K.H. Jürgen. In: Cahn RW, Flemings MC, Ilschner B, Kramer EJ, Mahajan S, Veyssière P, editors. *Encyclopedia of Materials: Science and Technology*. 2nd ed. Oxford: Elsevier; 2006;1–11.
18. Wang XH, Zhou YC. High-temperature oxidation behavior of Ti_2AlC in air. Oxid Met. 2003;59:303–20.
19. Pietzka MA, Schuster JC. Summary of constitutional data on the Aluminum-Carbon-Titanium system. J Phase Equilib. 1994;15:392–400.
20. Song GM, Schnabel V, Kwakernaak C, van der Zwaag S, Schneider JM, Sloof WG. High temperature oxidation behaviour of Ti_2AlC ceramic at 1200 C. Mater High Temp. 2012;29:205–9.
21. Kun L, Yuan Q, Ji-Zheng D. First-principles investigation of the vacancy effect on the electronic properties in M_2AlC (M = V and Nb). AIP Adv. 2014;4:107137.
22. Zhou Y, Sun Z. Electronic structure and bonding properties of layered machinable Ti_2AlC and Ti_2AlN ceramics. Phys Rev B. 2000;61:12570–3.

23. Wang XH, Zhou YC. Layered machinable and electrically conductive Ti_2AlC and Ti_3AlC_2 ceramics: a review. J Mater Sci Technol. 2010;26:385–416.

24. Li S, Song G, Kwakernaak K, van der Zwaag S, Sloof WG. Multiple crack healing of a Ti_2AlC ceramic. J Eur Ceram Soc. 2012;32:1813–20.

25. Yao F, Ando K, Chu MC, Sato S. Static and cyclic fatigue behaviour of crack-healed Si_3N_4/SiC composite ceramics. J Eur Ceram Soc. 2001;21:991–7.

26. Lee SK, Ono M, Nakao W, Takahashi K, Ando K. Crack-healing behaviour of mullite/SiC/Y_2O_3 composites and its application to the structural integrity of machined components. J Eur Ceram Soc. 2005;25:3495–502.

27. Kim BS, Ando K, Chu MC, Saito S. Crack-healing behavior of monolithic alumina and strength of crack-healed member. Zairyo/ J Soc Mater Sci Japan. 2003;52:667–73.

28. Potanin AY, Loginov PA, Levashov EA, Pogozhev YS, Patsera EI, Kochetov NA. Effect of mechanical activation on Ti_3AlC_2 MAX phase formation under self-propagating high-temperature synthesis. Eur Chem Technol J. 2015;17:233–42.

29. Barsoum MW, El-Raghy T, Ali M. Processing and characterization of Ti_2AlC, Ti_2AlN, and $Ti_2AlC_{0.5}N_{0.5}$. Metall Mater Trans A. 2000;31:1857–65.

30. Martienssen W, Warlimont H. *Springer Handbook of Condensed Matter and Materials Data*. Berlin, Heidelberg: Springer Science & Business Media; 2006.

31. Bei GP, Pedimonte BJ, Pezoldt M, Ast J, Fey T, Goeken M, et al. Crack healing in $Ti_2Al_{0.5}Sn_{0.5}C$-Al_2O_3 composites. J Am Ceram Soc. 2015;98:1604–10.

32. American society for testing of materials B311-93 Test method for density determination for powder metallurgy (P/M) materials containing less than two percent porosity. (International A); 1997.

33. Shimada S, Kozeki M. Oxidation of TiC at low temperatures. J Mater Sci. 1992;27:1869–75.

34. Chin Y-L, Tuan W-H, Huang J-L, Wang C-A. Toughening alumina with layered Ti_3SiC_2 inclusions. J Alloys Compd. 2010;491:477–82.

35. Chaubey A, Konda Gokuldoss P, Wang Z, Scudino S, Mukhopadhyay N, Eckert J. Effect of particle size on microstructure and mechanical properties of Al-based composite reinforced with 10 vol.% mechanically alloyed Mg-7.4%Al particles. Technologies. 2016;4:37.

36. Rattanachan S, Miyashita Y, Mutoh Y. Microstructure and fracture toughness of a spark plasma sintered Al_2O_3-based composite with $BaTiO_3$ particulates. J Eur Ceram Soc. 2003;23:1269–76.

37. Withers PJ. Fracture mechanics by three-dimensional crack-tip synchrotron X-ray microscopy. Philos Trans A Math Phys Eng Sci. 2015;373:20130157.

38. Ponnusami SA, Turteltaub S, van der Zwaag S. Cohesive-zone modelling of crack nucleation and propagation in particulate composites. Eng Fract Mech. 2015;149:170–90.

39. Barsoum MW, Radovic M. Elastic and mechanical properties of the MAX phases. Annu Rev Mater Res. 2011;41:195–227.

40. Auerkari P. Mechanical and physical properties of engineering alumina ceramics. Technical Research Centre of Finland, 1996 9513849872 Contract No.: Research Notes 1792.

41. Sloof WG, Pei R, McDonald SA, Fife JL, Shen L, Boatemaa L, et al. Repeated crack healing in MAX-phase ceramics revealed by 4D in situ synchrotron X-ray tomographic microscopy. Sci Rep. 2016;6:23040.

42. Cheng H, Dillon SJ, Caram HS, Rickman JM, Chan HM, Harmer MP. The effect of yttrium on oxygen grain-boundary transport in polycrystalline alumina measured using Ni marker particles. J Am Ceram Soc. 2008;91:2002–8.

43. Nanko M, Maruoka D, Sato Y. High-temperature oxidation of Y_2O_3-doped Al_2O_3 matrix composites dispersed with nano-Ni particles. Int J Appl Ceram Technol. 2012;9:172–7.

44. Pham HV, Maruoka D, Nanko M. Influences of Al_2O_3 grain size on high-temperature oxidation of nano-Ni/Al_2O_3 composites. J Asian Ceram Soc. 2016;4:120–3.

45. Mookhoek SD, Fischer HR, van der Zwaag S. A numerical study into the effects of elongated capsules on the healing efficiency of liquid-based systems. Comput Mater Sci. 2009;47:506–11.